
**Liquid Crystals**
Publication details, including instructions for authors and subscription information:
http://www.informaworld.com/smpp/title~content=t713926090

# Liquid crystalline properties of dissymmetric molecules part X: The effect of a terminal nitro group on molecular arrangement in smectic phases in three aromatic ring systems with two ester groups

Takeyasu Tasaka[a]; Hiroaki Okamoto[a]; Yuki Morita[a]; Kazuo Kasatani[a]; Shunsuke Takenaka[a]
[a] Department of Advanced Materials Science and Engineering, Faculty of Engineering Yamaguchi University Tokiwadai 2557 Ube, Yamaguchi 755-8611 Japan,

Online publication date: 11 November 2010

**To cite this Article** Tasaka, Takeyasu , Okamoto, Hiroaki , Morita, Yuki , Kasatani, Kazuo and Takenaka, Shunsuke(2003) 'Liquid crystalline properties of dissymmetric molecules part X: The effect of a terminal nitro group on molecular arrangement in smectic phases in three aromatic ring systems with two ester groups', Liquid Crystals, 30: 8, 961 — 977
**To link to this Article: DOI:** 10.1080/0267829031000139531
**URL:** http://dx.doi.org/10.1080/0267829031000139531

LIQUID CRYSTALS, VOL. 30, NO. 8, AUGUST, 2003, 961–977



# Liquid crystalline properties of dissymmetric molecules part X: The effect of a terminal nitro group on molecular arrangement in smectic phases in three aromatic ring systems with two ester groups†

TAKEYASU TASAKA, HIROAKI OKAMOTO*, YUKI MORITA, KAZUO KASATANI and SHUNSUKE TAKENAKA

Department of Advanced Materials Science and Engineering, Faculty of Engineering, Yamaguchi University, Tokiwadai 2557, Ube, Yamaguchi 755-8611, Japan

(*Received 28 October 2002; in final form 1 March 2003; accepted 1 April 2003*)

The smectic A (SmA) layer structure has been examined by X-ray diffraction for four isomeric systems: 4-nitrophenyl 4-(4-alkoxybenzoyloxy)benzoates **1**, 4-alkoxyphenyl 4-(4-nitrobenzoyloxy)benzoates **2**, 4-(4-alkoxybenzoyloxy)phenyl 4-nitrobenzoates **3**, and 4-alkoxyphenyl 4-nitrophenyl terephthalates **4**. The phase transition behaviour and layer structure of the SmA phases are notably influenced by the relative orientation of the two ester groups to the terminal groups, by alkoxy chain length, and by temperature. The SmA phase for compounds **1** and **3** has a mainly 'monolayer' arrangement, where the layer spacing is 2–5 Å longer than the molecular length. The SmA phase for compounds **2** and **4** consists of a mixed layer structure having monolayer, bilayer, and partially bilayer arrangements, the distribution depending on the relative orientation of the ester groups, the alkoxy chain length, and temperature. It is supposed that the diversity of the SmA phase is related to the polar interaction around the nitro or the nitrobenzene moieties through the smectic layers and reversal of the ester groups causes a subtle change in the entire molecular shape.



## 1. Introduction

In an earlier paper, we showed that in three isomeric systems: 4-*R*-phenyl 4-(4-octyloxybenzoyloxy)benzoates, 4-octyloxyphenyl 4-(4-*R*-benzoyloxy)benzoates, and 4-octyloxyphenyl 4-*R*-phenyl terephthalates ($R$ = halogens, $CF_3$, $OCF_3$, etc.), properties such as the smectic A (SmA)–nematic (N) or SmA–isotropic (I) transition temperatures, and the layer structure of the SmA phase, are influenced by the physical properties of the terminal substituents. Interestingly, the layer spacing of most SmA phases is always longer by 2–4 Å than the molecular length for the most stable conformation calculated by a semi-empirical molecular orbital calculation. Based on these results, we proposed a new molecular arrangement model for the SmA phase exhibited by dissymmetric liquid crystal (LC) molecules, where the substituents cohere around the surface of the smectic layer, as shown in figure 1 [1]. For this formation, phase separation between a polar segment, i.e. the substituted benzene moiety, and a non-polar segment, i.e. the alkoxy chain is supposed to be a driving force.

The SmA phase exhibited by LC molecules having a very polar terminal group, such as nitro or cyano, is supposed to have peculiar thermal properties and layer structure. For example, LC materials containing a two-ring system such as 4-*R*-4′-cyanobiphenyl and 4-cyanophenyl 4-*R*-benzoate, and 4-cyanobenzylidene-4-*R*-aniline compounds ($R$ = *n*-alkyl or *n*-alkoxyl) are known to form a peculiar anti-parallel dimer, and the higher homologues exhibit an SmA phase ($SmA_d$) where the layer spacing is frequently *c*. 1.4–1.5 times the molecular length. For this $SmA_d$ phase, segments of the LC molecules are assumed to arrange side by side, giving a 'partially bilayer' arrangement [2]. The layer structure of the SmA phase exhibited by polar LC materials is classified into three main kinds; monolayer, bilayer, and partially bilayer, denoted, $SmA_1$, $SmA_2$, and $SmA_d$, respectively, according to the conventional classification [3].

In particular, the $SmA_1$ phase exhibited by polar LC materials is termed a 'polar' $SmA_1$ phase, where the

*Author for correspondence; e-mail: oka-moto@po.cc.yamaguchi-u.ac.jp

†For part IX see ref. [4].

*Liquid Crystals* ISSN 0267-8292 print/ISSN 1366-5855 online © 2003 Taylor & Francis Ltd
http://www.tandf.co.uk/journals
DOI: 10.1080/0267829031000139531

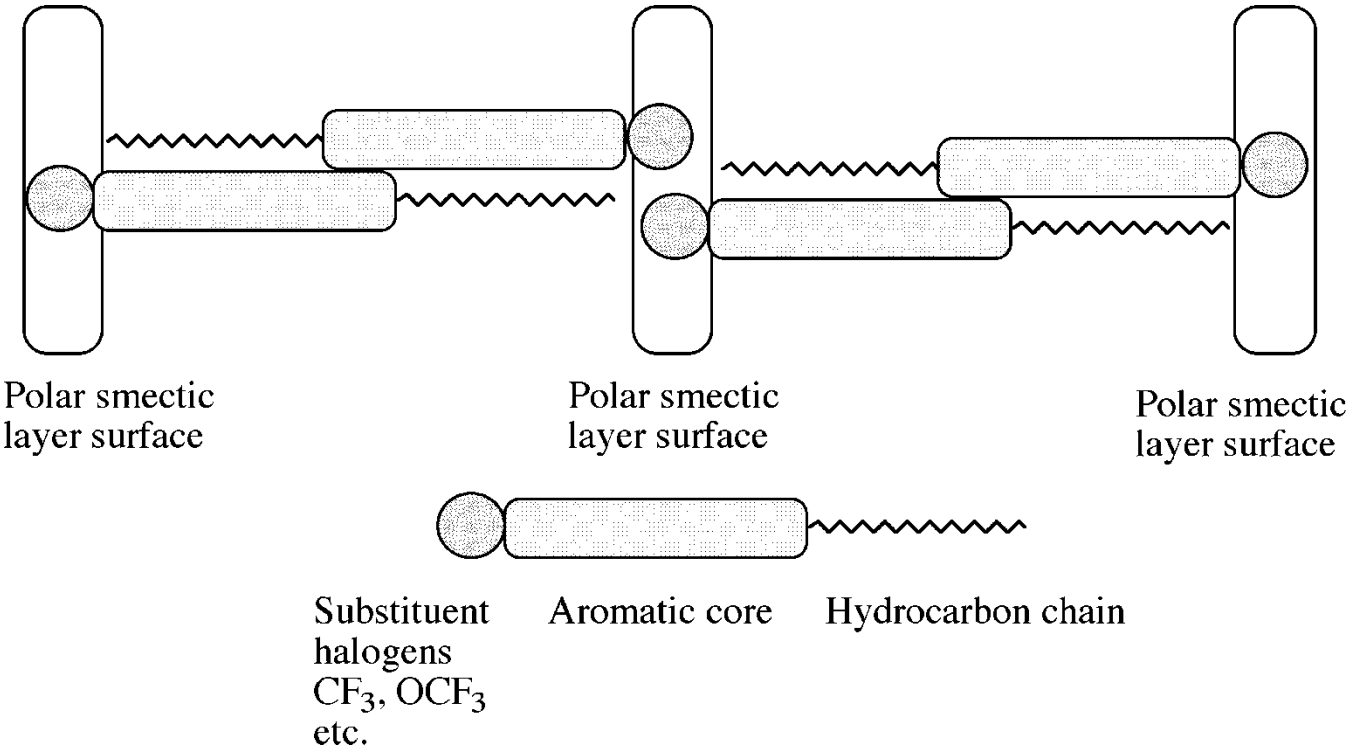


Figure 1. Molecular arrangement model for the SmA phase of dissymmetric LC molecules.

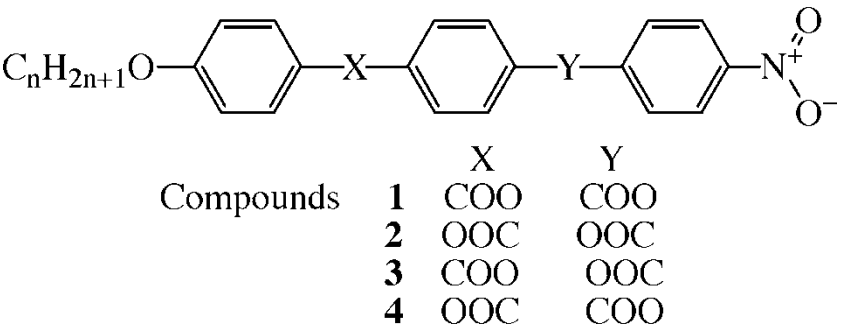


| Compounds | | X | Y |
|---|---|---|---|
| | **1** | COO | COO |
| | **2** | OOC | OOC |
| | **3** | COO | OOC |
| | **4** | OOC | COO |

Figure 2. Molecular structures of compounds **1**–**4**.

layer spacing is always greater than the expected molecular length. The molecular arrangement of the polar $SmA_1$ phase may correspond to that of the dissymmetric LC materials shown in figure 1.

We have been interested in the correlation between the 'polar' $SmA_1$ phase and the SmA phase exhibited by dissymmetric LC materials. In our previous paper, it was reported that a homologous series of 4-nitrophenyl 4-(4-alkoxybenzoyloxy)benzoates, exhibit the SmA phase beginning from the hexyloxy homologue, and the layer spacing is 2–5 Å longer than the calculated molecular length [4]. From these results, the SmA phase at the lower temperature region has been supposed to have a similar layer structure to that in figure 1.

This compounds have four kinds of isomer, **1**–**4**, with respect to the relative orientation of the terminal alkoxy and nitro groups, as shown in figure 2. These would be very suitable materials for clarification of the effect of physical properties of materials on LC properties.

Accordingly, we re-examined the layer structure of the SmA phase for **1**–**4**. Some of the homologues have already been prepared, and the layer structure of their SmA phase examined [5–13]. For example, the hexyloxy homologue of **1** exhibits the SmA phase, where the layer spacing is a little longer than the

calculated molecular length [6]. The octyloxy homologue of **2** is known to exhibit a SmA phase classified as the $SmA_1$ modification [11]; the nonyloxy and decyloxy homologues exhibit a complex polymesomorphism involving plural SmA and smectic C (SmC) phases [12, 13]. In this paper, we wish to re-consider the smectic properties of the four isomeric compounds in connection with (i) the effect of the terminal nitro group, (ii) replacement of two ester groups, (iii) terminal alkoxy chain length, and (iv) temperature dependency.

## 2. Experimental

### 2.1. *Materials*

The homologous series **1**–**4** were prepared by the conventional method described in our earlier paper [5]. The purity of compounds **1**–**4** was checked by $^1$H NMR spectroscopy (JEOL, EX-270) and HPLC (Shimadzu, C-R4XA) where an ODS column was used.

### 2.2. *Methods*

The transition temperatures and latent heats were determined using a differential scanning calorimeter (DSC) Seiko SSC-5200, with indium (99.9%) as calibration standard (m.p. = 156.6°C, 28.4 J g$^{-1}$). The DSC thermogram was operated at heating or cooling rates of 5°C min$^{-1}$. The mesophases were characterized using a Nikon POH polarizing microscope fitted with a Mettler thermo-control system (FP-900), calibrated with benzoic acid (m.p. = 122.4°C).

X-ray diffraction (XRD) measurements for the SmA phase were performed using a Rigaku-Denki RINT 2200 diffractometer, with $CuK_\alpha$ ($\lambda = 1.541$ Å) as X-ray source. The reflection angle was calibrated by a comparison of both the right and left angles; the temperature was controlled using a Rigaku PTC-20A thermo-controller. The sample was filled into the quartz capillary (diam. = 1.5 mm) and oriented by a constant magnetic field (480 G). The sample was placed along the goniometer axis so that the counter movement in the recording plane allowed us to scan the nematic and smectic reciprocal lattice mode along $q$ ($q = 2p/d$ is the reciprocal space vector), i.e. in the direction parallel to the director **n**. Heating the sample to 200°C sometimes gave a complex X-ray profile, probably due to decomposition, and reproducibility was lost. Therefore, the sampling and XRD were carried out below 200°C. The X-ray profiles were recorded as an integrated (30 times) average in the range between −5° and 20° (scan speed: 3° min$^{-1}$).

The molecular orbital parameters referenced in this paper were obtained by a semi-empirical molecular orbital calculation, MOPAC97, where minimization of the heat of formation was achieved by an AM1 method.

Table 1. Transition temperatures (°C) of compounds **1**–**4**. Cr, SmA, N, and I indicate crystal, smectic A, nematic, and isotropic phases, respectively.

| Compound | *n* | Cr | | SmA | | N | | I | R[a] |
|---|---|---|---|---|---|---|---|---|---|
| **1a** | 7 | • | 113 | • | 198 | • | 230 | • | 0.93 |
| **1b** | 8 | • | 114 | • | 210 | • | 224 | • | 0.97 |
| **1c** | 9 | • | 116 | • | 218 | • | 222 | • | 0.99 |
| **1d** | 10 | • | 116 | • | 224 | — | | • | 1.0 |
| **2a** | 7 | • | 88 | • | 127 | • | 228 | • | 0.80 |
| **2b** | 8 | • | 101 | • | 129 | • | 228 | • | 0.80 |
| **2c** | 9 | • | 100 | • | 195 | • | 224 | • | 0.94 |
| **2d** | 10 | • | 89 | • | 208 | • | 220 | • | 0.98 |
| **3a** | 7 | • | 160 | • | 226 | • | 248 | • | 0.96 |
| **3b** | 8 | • | 165 | • | 239 | • | 246 | • | 0.99 |
| **3c** | 9 | • | 165 | • | 242 | • | 243 | • | 1.0 |
| **3d** | 10 | • | 159 | • | 248 | — | | • | 1.0 |
| **4a** | 7 | • | 159 | — | | • | 220 | • | |
| **4b** | 8 | • | 153 | • | 190 | • | 220 | • | 0.90 |
| **4c** | 9 | • | 156 | • | 198 | • | 219 | • | 0.96 |
| **4d** | 10 | • | 155 | • | 200 | • | 220 | • | 0.96 |

[a]McMillan parameter, ref. [15].

## 3. Results and discussion

### 3.1. *Thermal properties*

The melting points, SmA–N(I) and N–I transition temperatures observed by DSC for the proposed homologues of compounds **1**–**4** are summarized in the table, where the complex polymesomorphism exhibited by the higher homologues of **2** are omitted [12, 13]. Transition temperatures are plotted against carbon number ($n$ = length of alkoxy chain) in figure 3, where the transition temperatures are cited from references [4, 5].

4-Octyloxyphenyl 4-(4-alkoxybenzoyloxy)benzoates, the derivatives of **1** having an octyloxy group instead of the nitro group, were reported to exhibit SmA and SmC phases starting from the earlier homologues [14]; the tendency is inherited by the nitro homologues of **1**, where the SmA phase commences at $n = 6$. For the pentyloxy homologue, cybotactic domains having a layer structure like the SmA phase exist in the N phase [4]. As shown in the table, the ratio of the SmA–N to N–I transition temperatures for the homologues of **1** is high [15].

4-Alkoxyphenyl 4-(4-octyloxybenzoyloxy)benzoates, the derivatives of **2** having an octyloxy group instead of the nitro group, also exhibit SmA and SmC phases, while the SmC(A)–N transition temperature is quite low [14]. For the nitro compounds **2**, similarly, the SmA–N transition temperature for the homologues ($n$ = 5–8) is lower, and the ratio of the SmA–N to N–I transition temperatures is low.

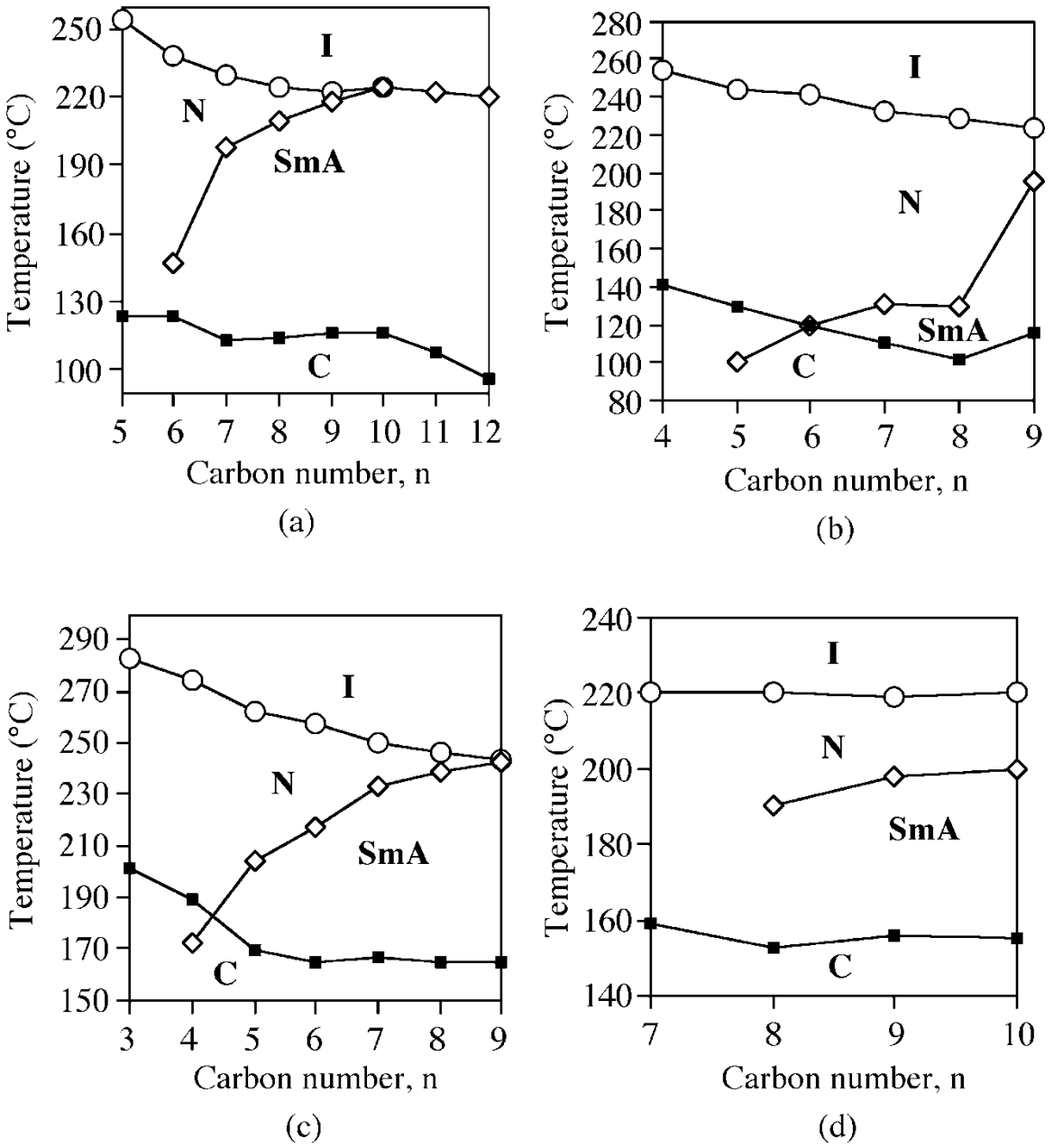


Figure 3. Plots of transition temperature vs. carbon number $n$: (*a*) **1**, (*b*) **2**, (*c*) **3**, (*d*) **4**. (○) N–I, (◇) SmA–N(I), (■) melting point; the SmA–N transition below the melting point is a monotropic process.

4-Octyloxybenzoyloxyphenyl 4-alkoxybenzoates the derivatives of **3** having an octyloxy group instead of the nitro group, do not exhibit an SmA phase, even in the higher homologues, and only an SmC phase is seen in the higher homologues [14]. In contrast, the nitro homologues of **3** readily exhibit the SmA phase, beginning from $n=4$, and the SmA–N transition temperature gradually increases on ascending the homologous series. Apparently, the terminal nitro group facilitates the formation of the SmA phase and increases the SmA–N transition temperature.

4-Octyloxyphenyl 4-alkoxyphenyl terephthalates, the derivatives of **4** having an octyloxy group instead of the nitro group, exhibit both SmA and SmC phases [14]. In contrast, compounds **4** do not readily exhibit the SmA phase, which only commences from the octyloxy homologues the ratio of the SmA–N to N–I transition temperature is rather low.

From these results, it is concluded that the terminal nitro group does not always enhance the smectic properties, as compared with trifluoromethyl, trifluoromethoxy groups, and some halogens [1].

It has been reported that some homologues of **1**–**4** show complex phase transition behaviour in addition to the SmA–N transition in the table. For example, the mesomorphism for **2c** was reported to be [12, 13]: $SmC_2 \cdot 96 \cdot SmA_2 \cdot 100 \cdot SmC \cdot 119 \cdot SmA_1 \cdot 121.5 \cdot N_{re} \cdot 124 \cdot SmA_d \cdot 138.5 \cdot N_{re} \cdot 156 \cdot SmA_d \cdot 195 \cdot N$ (°C). The existence of another SmC phase between $SmA_1$ and SmC was also reported [11]. Compound **2d** also exhibits complex phase transition behaviour, [16]: SmC(1)·99·SmA(3)·117·SmA(2)·125·SmA(1)·208·N·219·I (°C).

### 3.2. *X-ray diffraction studies*

The SmA phase was further characterized by X-ray measurement. The X-ray profiles for **1b** are illustrated in figure 4. All the profiles also have a broad and a weak reflection peak near $2\theta = 20°$, not shown in the figure. The profile at 190°C shows a sharp reflection peak at $2\theta = 2.46°$ corresponding to 35.9 Å. The reflection peak shifts a little to the wide angle region and intensifies with decreasing temperature. Although the pentyloxy homologue of **1** does not exhibit the SmA phase under microscopic and DSC observation, the X-ray profiles show a broad reflection centered at 3.1° (28.1 Å) in the range 150–120°C (crystallization point), and the peak gradually intensifies. These results suggest that cybotactic domains having a SmA-like layer structure exist in the N phase.

The layer spacing calculated from the reflection peak is plotted against temperature in figure 5. Layer spacing is a function of carbon number, and stays almost constant throughout the temperature range. Shashidhar *et al.* have already reported that the layer spacing for the hexyloxy homologue remains constant throughout the SmA range [6, 17].

Compounds **2** show a fairly complex XRD pattern and temperature dependency. As an example, the X-ray profiles for **2a** are given in figure 6. At 122°C, less than 5°C from the SmA–N transition point, the profile shows a sharp peak at $2\theta = 3.10°$ (28.5 Å), and a broad peak centred at $2\theta = 1.76°$ (50.2 Å). The latter broad peak becomes sharp and intense, and simultaneously

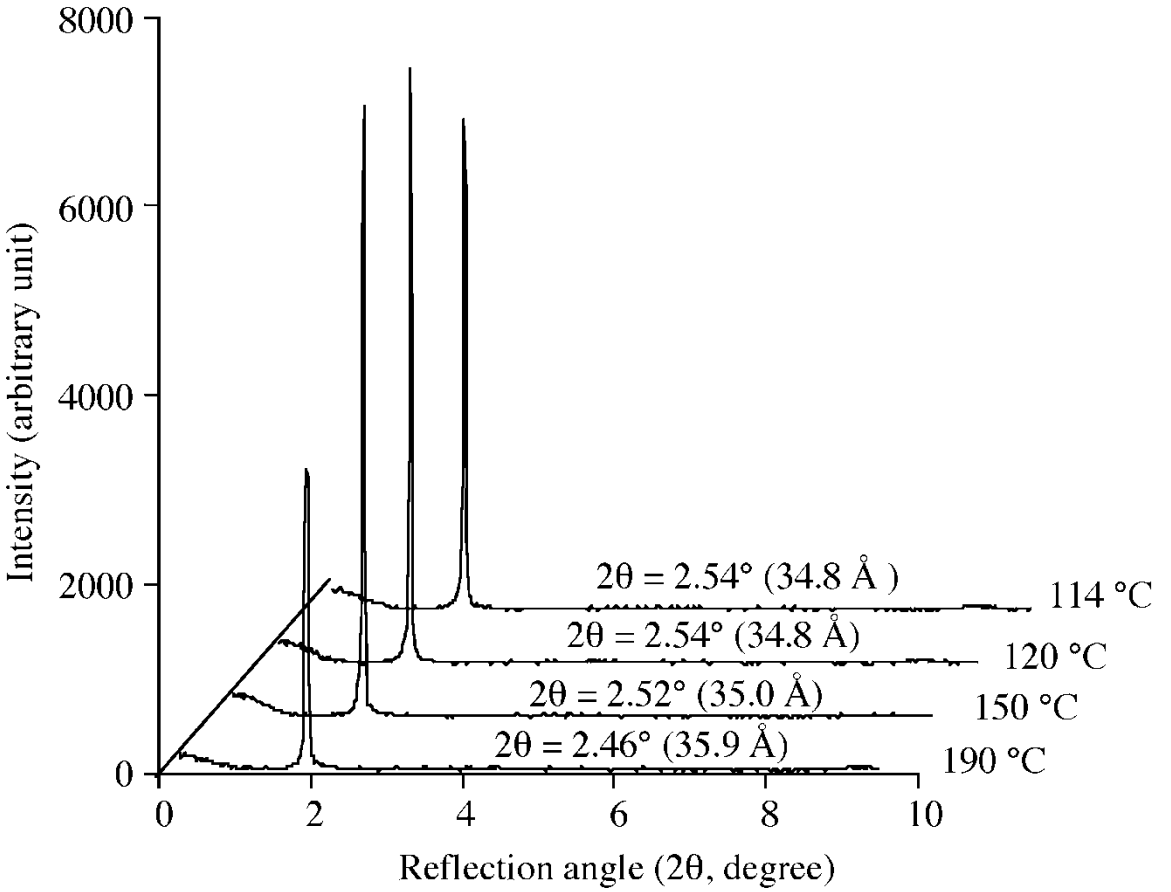


Figure 4. X-ray profiles for **1b** in the SmA phase.

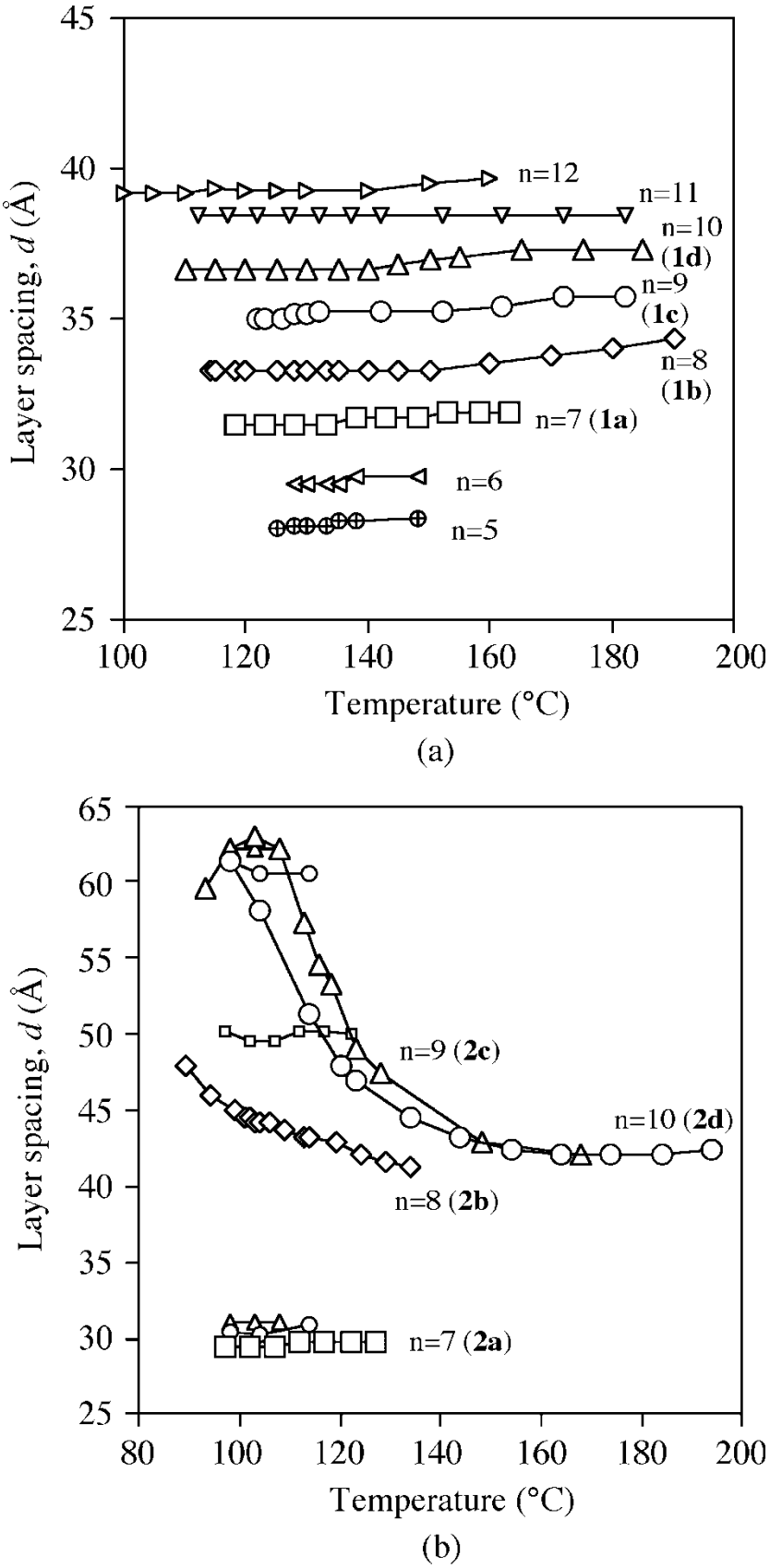


Figure 5. Plots of the layer spacing vs. temperature: (*a*) compounds **1**, (*b*) compounds **2**. Small □, △, and ○ indicate the alternative layer spacing for **2a**, **2c**, and **2d**, respectively; see figures 6 and 7.

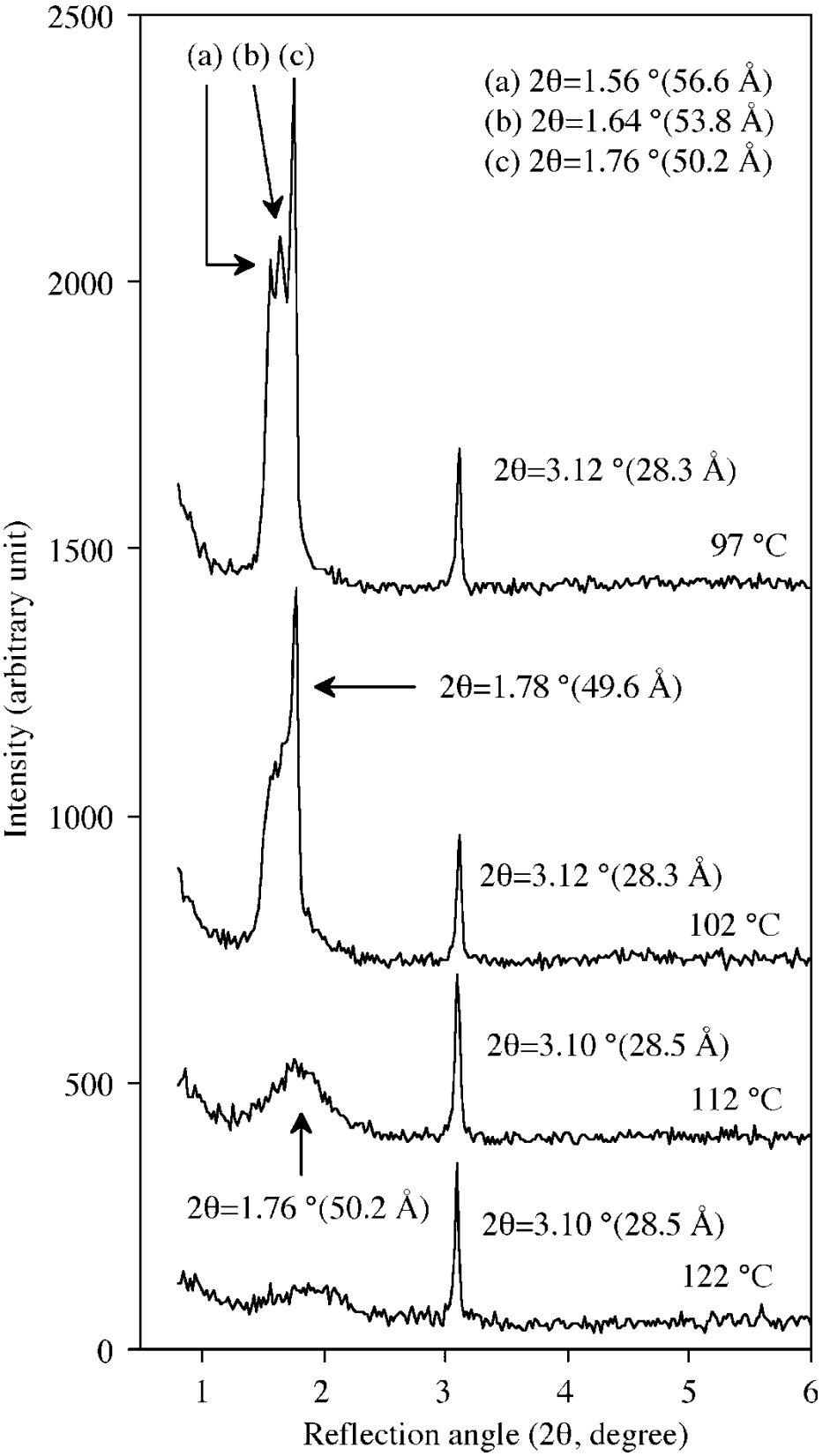


Figure 6. X-ray profiles for **2a** in the SmA phase.

the former becomes weak with decreasing temperature (for example, at 112°C in the figure). Thereby, the intensity ratio of the latter to the former is 1:1.5, 1:3, 1:7, and 1:10 at 122, 112, 102, and 97°C, respectively. Furthermore, the peak at $2\theta = 1.78°$ at 102°C splits into three at $2\theta = 1.76°$, 1.64°, and 1.56° at 97°C. These results indicate that the SmA phase consists of a mixture of various layer structures having a different layer spacings, and the distribution is a function of temperature. Thus, the layer structure having a spacing of $2\theta = 3.10°$ (28.5 Å) exists over the whole range and becomes dominant in the lower temperature region. The peak at $2\theta = 1.56°$ (56.6 Å) corresponds to just twice the spacing of the peak at $2\theta = 3.10°$ (28.3 Å).

Compound **2b** shows only one reflection peak throughout the temperature range. The profiles at 150°C, over 21°C from the SmA–N transition, show a broad and weak maximum centered at $2\theta = 2.20°$ (40.1 Å), and the peak gradually shifts to the narrow angle region with decreasing temperature. In the range between 111 and 109°C, the peak at $2\theta = 2.02°$ (43.7 Å) steeply intensifies without changing its position.

The profiles for **2c** are shown in figure 7. In the range 194–120°C, the profile shows an intense peak at 2.38° (47.0 Å), and a weak and broad reflection peak near 2°. In the range 122–111°C, the former peak shifts to $2\theta = 1.79°$ (49.1 Å) with decreasing temperature, and a new sharp reflection peak emerges at $2\theta = 1.44°$ (61.3 Å) from the broad peak and another new peak appears at $2\theta = 2.90°$ (30.4 Å). These two peaks intensify with decreasing temperature without changing their positions. The profile at 98°C shows two peaks at $2\theta = 1.44°$ (61.3 Å) and 2.90° (30.4 Å), where the intensity ratio of the former to the latter is 10:1. These results suggest that some layer structures coexist in the range 120–100°C, and that their distribution is a function of temperature.

Shashidhar *et al.* reported that the reflection peak at 2.38° (47.0 Å) shows a low angle shift with decreasing temperature and disappears near 120°C; then a new reflection peak appears near 2.9° and the angle is almost independent of temperature [12]. The discontinuous change has been correlated with the complex phase transition behaviour observed by microscopy. The replacement of the higher temperatures peak at $2\theta = 2.38°$ by the lower temperature peak at $2\theta = 1.44°$, may correspond to the discontinuous change. Compound **2d** shows a similar feature, where the reflection peak at 2.10° (42.0 Å) at 168°C continuously shifts to a narrow angle region with decreasing temperature, and then to a wide angle peak on further decreasing the temperature, giving a maximum of $2\theta = 1.40°$ (63.1 Å) at *c.* 110°C, as shown in figure 5 (*b*). The reduction of the layer spacing at the low temperature region should be related to the evolution of the SmC (SmC2) phase. Compound **2d** simultaneously exhibits a weak reflection peak at 2.84° (31.3 Å) below 113°C, where the intensity ratio of the peak at 1.42° (62.2 Å) to that at 2.84° is 100:8 at 98°C. It has been reported that for **2d**, the reflection peak shows a continuous change with temperature and gives a minimum around 150–170°C [16]. The present results shown in figure 5 (*b*) agree well with the phenomena reported in the literature.

The homologues of **3** have high SmA–N or I transition temperatures. The samples could not be heated to the SmA–N or the N–I transition point and annealed for 20 min without decomposition; in addition the X-ray measurement was carried out below 190°C, so that the molecular alignment in the capillary may not be sufficient. Under these conditions, the X-ray profiles for all the homologues of **3** show one reflection peak near 2.5–3.0°, and the profiles for **3b** are illustrated as an example, in figure 8.

The reflection peak at $2\theta = 2.74°$ (32.2 Å) is accompanied by a broad shoulder in the range $2\theta = 2.4$–$2.7°$, while it does not separate as any independent peak(s) even in the lower temperature region. Apparently, the layer spacing for **3b** stays almost constant throughout the temperature range. A similar feature was observed for the other homologues. The layer spacing is plotted in figure 9. The X-ray profiles for **4b** are shown in figure 10. The profiles above 162°C show one peak at 2.32° (38.0 Å), which intensifies without changing the reflection angle with decreasing temperature. The profiles below 155°C also show new peaks at $2\theta = 2.66°$ (33.2 Å) and $2\theta = 2.30°$ (38.5 Å), where the intensity ratio of the latter to the former is 100:23 at 155°C. Although the reflection angle of both peaks stays constant, the intensity ratio changes to 100:59 at 150°C. These results indicate that two layer structures coexist in the Sm A phase, and the distribution of the two states is a function of temperature. Compounds **4c** and **4d** show a similar phase behaviour. The temperature dependency of the layer spacing is shown in figure 9 (*b*).

In order to analyse the X-ray results more exactly, the molecular shapes and lengths were estimated by molecular orbital calculations, where a semi-empirical molecular orbital method (MOPAC97) was used; the heats of formation were minimized by an AM1 method. Polarity and shape of compounds **1**–**4** vary due to the relative orientation of the two ester groups, the terminal nitro and alkoxy groups; the alkoxy chain length also affects the entire molecular shape [14]. In the calculation, we assumed that the terminal alkoxy chain takes a zigzag conformation, to give the best linearity of the whole molecular shape. The two ester groups are assumed to have an *s-trans* conformation to

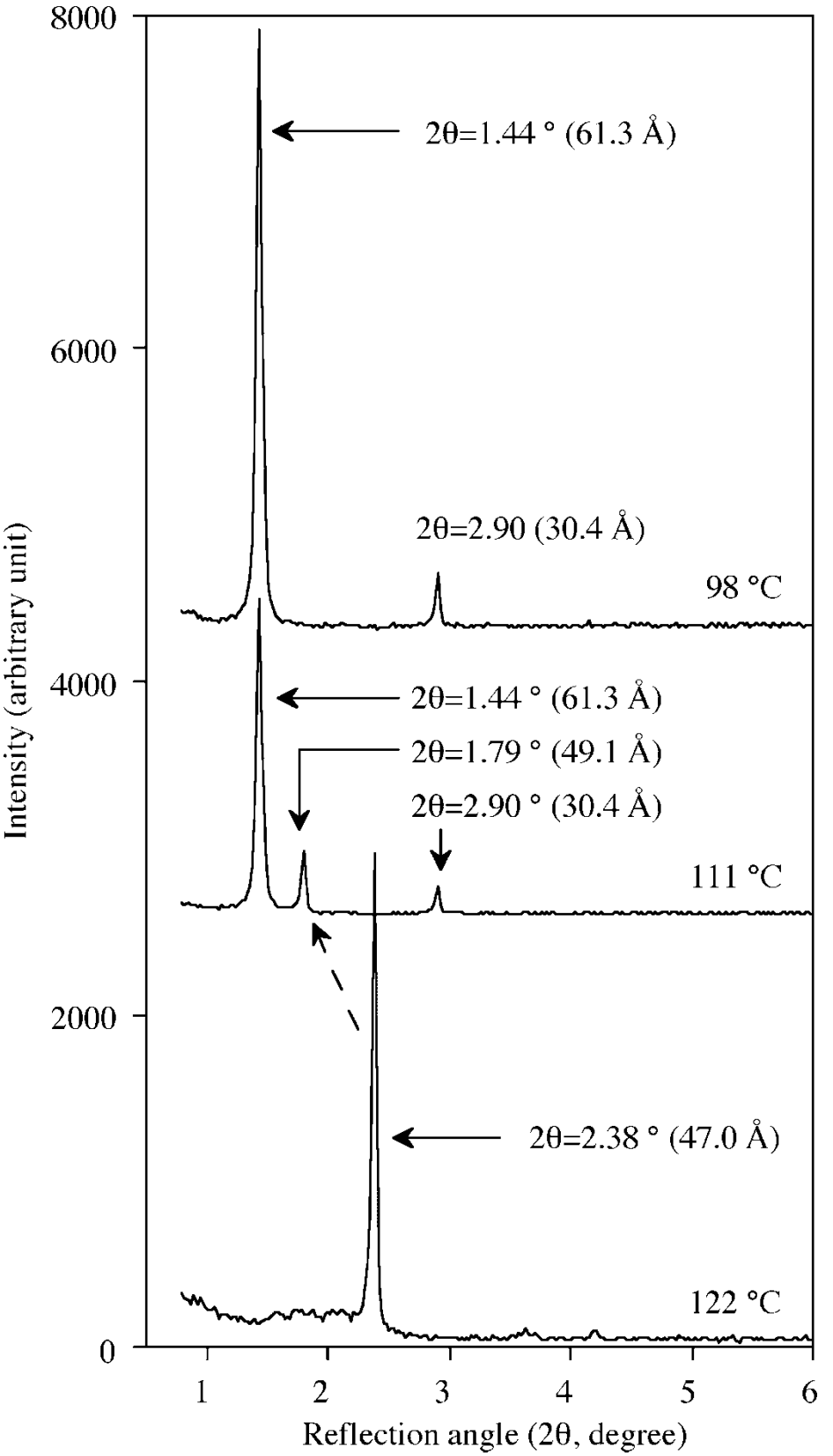


Figure 7. X-ray profiles for **2c** in the SmA phase.

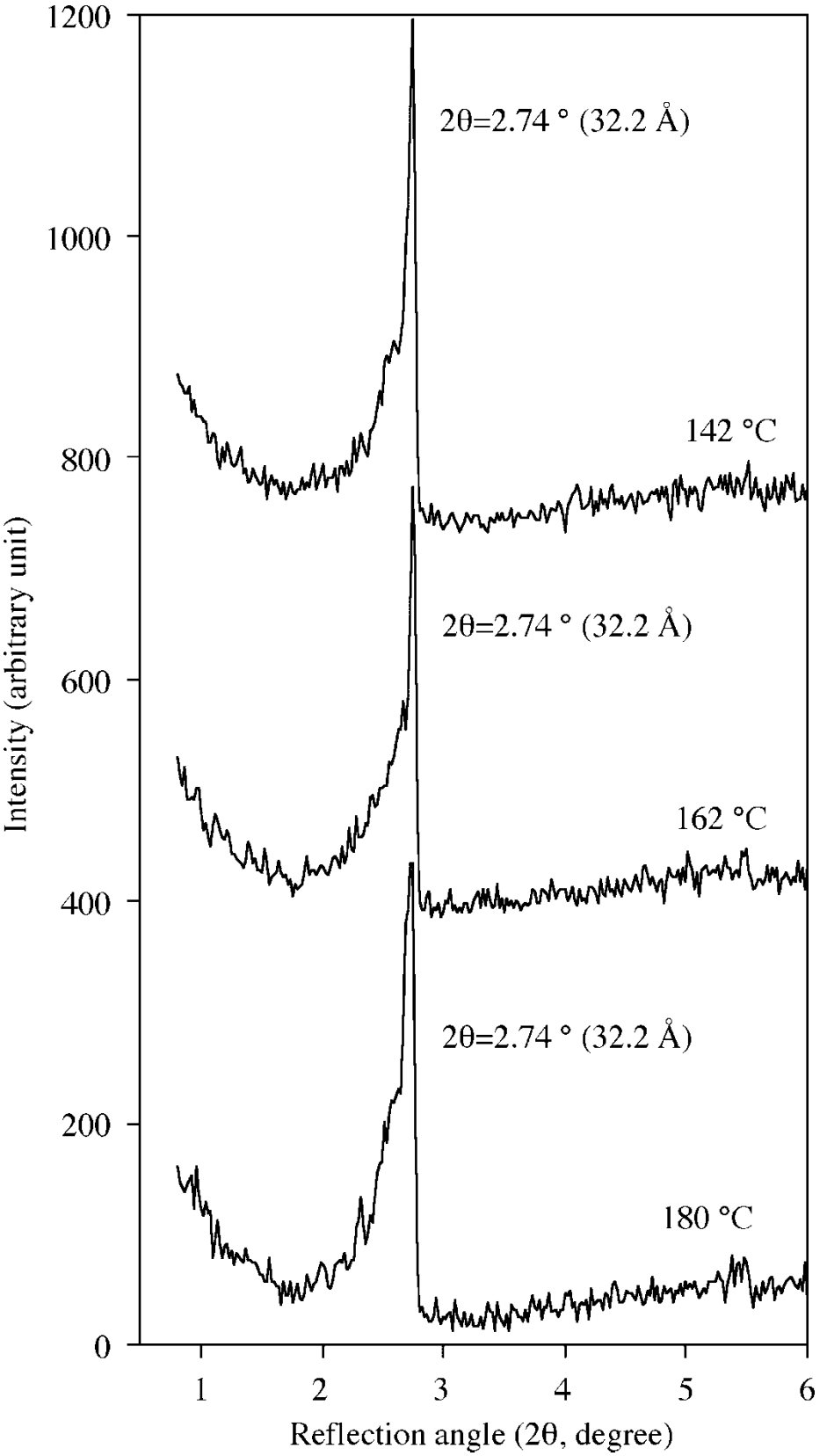


Figure 8. X-ray profiles for **3b** in the SmA phase.

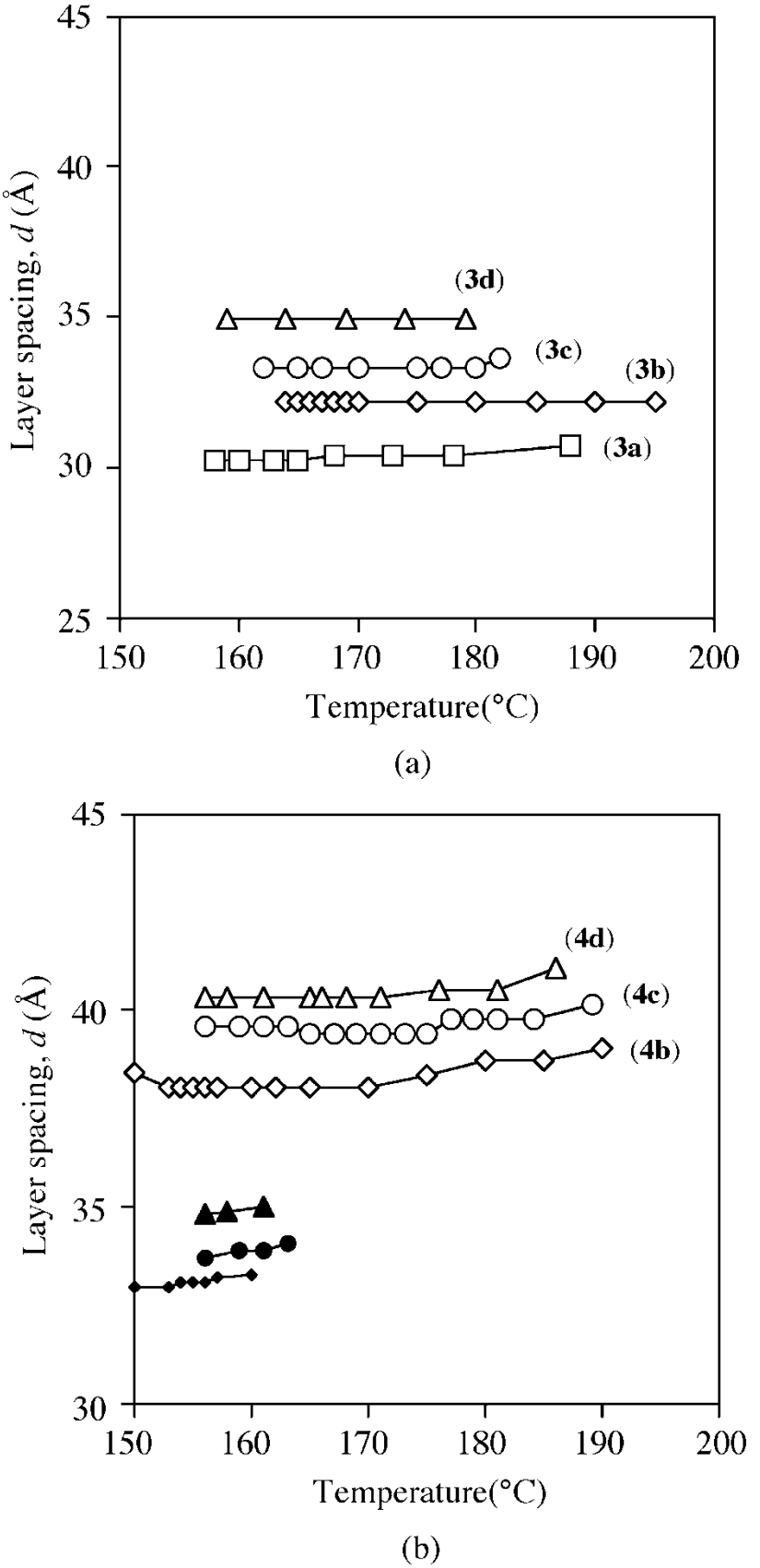


Figure 9. Plots of the layer spacing vs. temperature: (*a*) compounds **3**, (*b*) compounds **4**. ◆, ●, and ▲ indicate minor reflection peaks for **4b**, **4c** and **4d**, respectively.

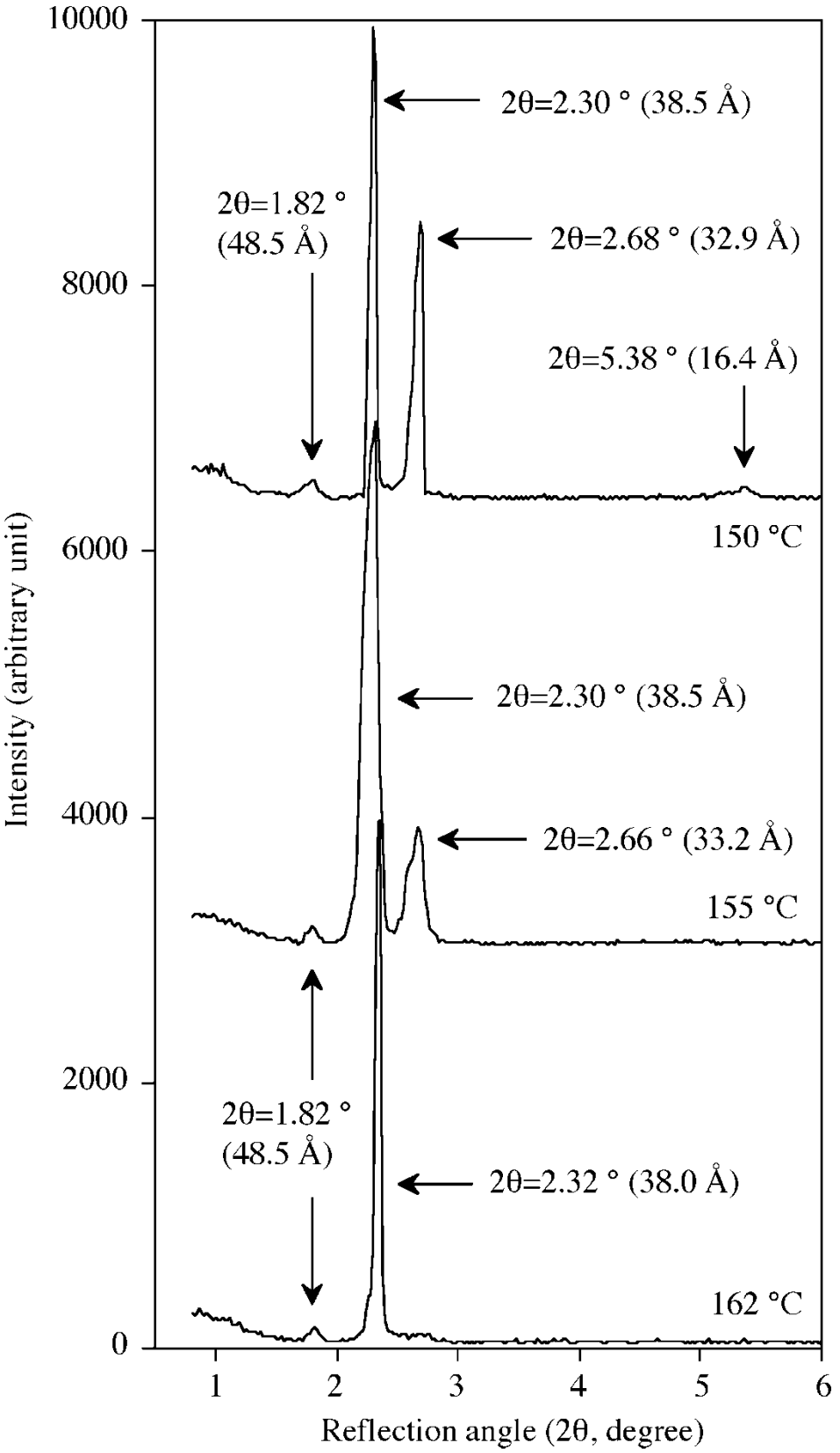


Figure 10. X-ray profiles for **4b**.

each other, to maintain the linearity of the core portion, although *trans*- and *cis*-conformations are almost equivalent in energy and might co-exist in the LC states and isotropic solution. We have previously reported that for non-polar LC materials, the molecular length calculated under these assumptions is in good agreement with the observed layer spacing of the SmA phase [14]. For example, the molecular structures in figure 11 represent the most stable conformations for **1**, **2**, and **4**. The molecular lengths of **1**–**4** for the most stable conformation are plotted against the carbon number $n$, in figure 12.

If the molecules form only a monolayer arrangement, and the average axis of the alkoxy chain arranges orthogonal to the layer plane, the observed layer spacing should simply increase, giving a slope of 1.25 Å per $CH_2$ unit. In our earlier paper, it was confirmed that four analogues of **1**–**4**, substituted by alkyl and/or alkoxyl groups instead of the terminal nitro group, exhibit a SmA phase having a monolayer arrangement, where the layer spacing is in good agreement with the calculated molecular length, and the slope is 1.2 Å/$CH_2$ [14].

On the other hand, supposing that the molecules form a tight anti-parallel dimer, e.g. figure 11 (*c*), the slope is expected to be twice (2.5 Å/$CH_2$). Certainly, for the $SmA_d$ phase of 4-alkoxyphenyl 4-cyanobenzoates, the layer spacing is given by $d$Å $= 2.58n + 19$ ($n$ is the carbon number of the alkoxy chain), where the constant value of 19 Å corresponds to the distance across the LC core of the dimer [18].

In figure 12 (*a*) the layer spacing for **1** shows a linear correlation against the carbon number, where the plot is given by $d$Å $= 1.67n + 19.7$, and the calculated molecular length is given by $l$Å $= 1.24n + 19.7$ [4]. Interestingly, both lines intersect at $n = 1$, where the extrapolated layer spacing is 21.0 Å, agreeing with the calculated diameter of the methoxy homologue. Assuming that the methoxy homologue of **1** forms the SmA phase, its molecules are expected to have the anti-parallel arrangement shown in figure 12 (*a*).

In figure 12 (*a*) the nitro groups protrude little from the smectic layer, and the aromatic cores arrange side by side within the smectic layer. This model corresponds to our smectic model in figure 1 [1]. For the homologous series **1**, in practice, the methoxy–butoxy homologues do not exhibit the SmA phase, which commences at the hexyloxy homologue. For the pentyloxy homologue, as mentioned above, cybotactic domains having a layer structure exist in the N phase, though they could not be observed by DSC or microscopy. Interestingly, the layer structure in the domains has a spacing of 28.2 Å, and the plot fits on the average line, as indicated by a black circle in figure 12 (*a*).

R. Shashidhar *et al*. reported that the layer spacing of the SmA phase for the hexyloxy homologue is a little longer than the calculated molecular length, and almost independent of temperature. In addition, they classified the SmA phase as the $SmA_d$ modification, and the homologue potentially has a reentrant N phase [17]. Indeed, the layer spacing for the hexyloxy and higher homologues is insensitive to temperature change, as shown in figure 5 (*a*).

Two extreme molecular arrangement models of the SmA phase for the octyloxy homologue are illustrated in figures 11 (*b*) and 11 (*c*), namely $SmA_1$(polar) and $SmA_d$, respectively, where $\Delta$ indicates the difference between the layer spacing and calculated molecular length. The model in figure 11 (*c*) is the most popular and frequently used for the layer structure of the $SmA_d$ phase, where the layer spacing is *c*. 1.5 times the molecular length. For the layer structure, the LC core portions arrange anti-parallel and overlap side by side. Inevitably, the layer surface is covered with terminal alkoxy groups, giving a non-polar layer boundary. As one can see from the figure, however, the nitro groups are more than 15 Å apart, so that the polar interactions may be too weak to keep the anti-parallel arrangement. In the $SmA_1$ model in figure 11 (*b*), on the other hand, there is a small gap between neighbouring LC cores, and the nitro groups cohere around the layer boundary. In such conditions, the nitro groups come close enough to each other to maintain the anti-parallel arrangement throughout the smectic layers.

Considering these facts, the model in figure 11 (*b*) may be probable for the SmA phase for **1** where, of course, $\Delta$ is a function of the terminal alkoxy chain length. Conclusively, the SmA phase for **1** has a monolayer structure ($SmA_1$), while the distribution of the $SmA_d$ structure increases with increasing temperature and alkoxy chain length, as pointed by Shashidhar *et al*. [6].

The reflection peaks for **2** in figure 12 (*b*) can be divided into three kinds. One peak appeared near 60 Å, close to twice the molecular length. For example, the maximum layer spacings for **2c** and **2d** are 61.3 and 63.0 Å, corresponding to 2.00 and 1.99 times the calculated molecular lengths, respectively. Interestingly, this type of peak is not observed in **2b**, while it is observed in the low temperature region in **2a**. Second is the reflection peak near 30 Å close to the calculated molecular length. Third lies in the range between 40 and 50 Å. The reflections for **2c** and **2d** continuously shift to *c*. 60 Å at the low temperature region. These results indicate that three kinds of layer structures co-exist and interact each other in the smectic region; a

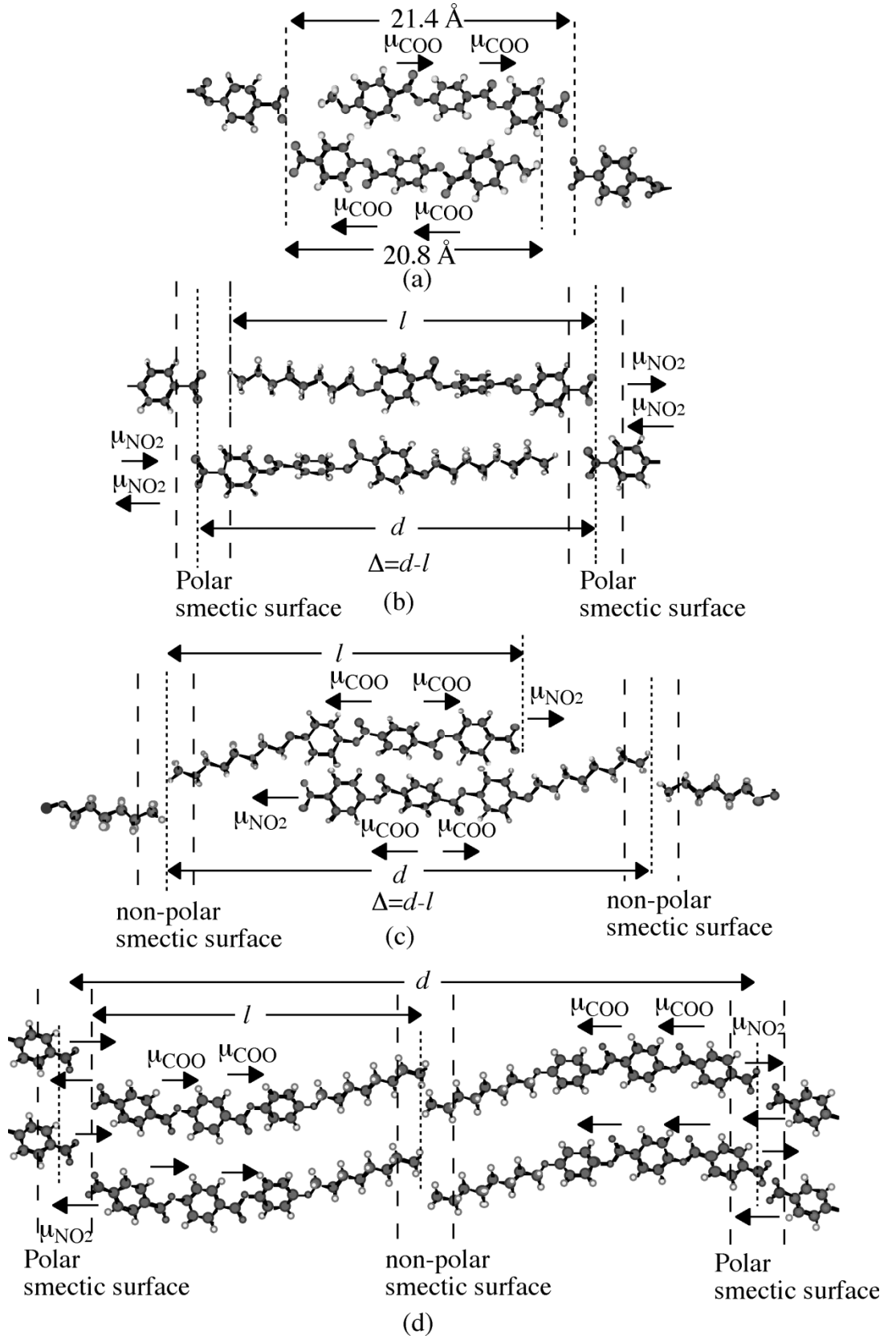


Figure 11. Possible molecular arrangements in the SmA phase: for details see text.

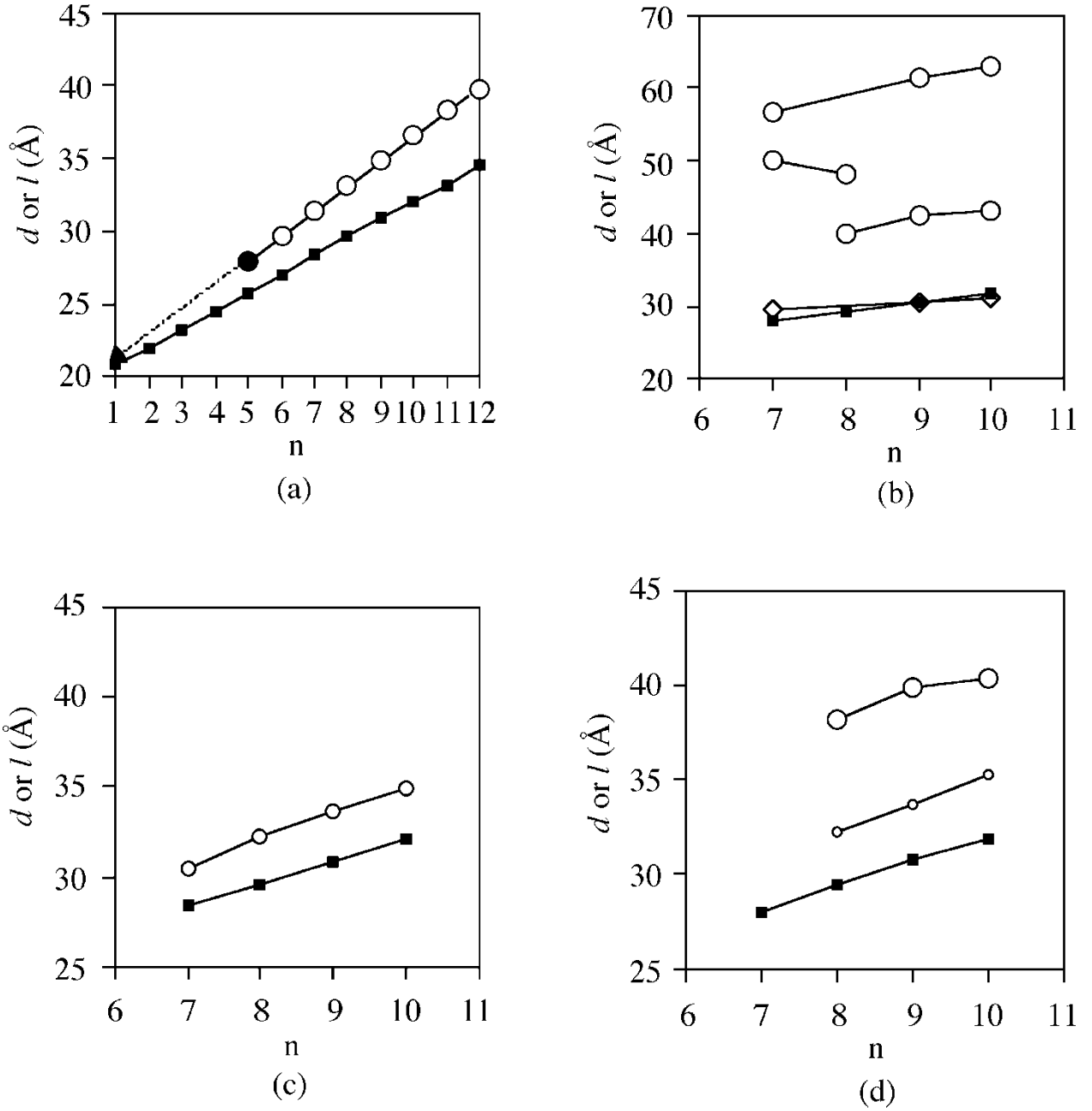


Figure 12. Plots of layer spacings $d$ and molecular lengths $l$ vs. carbon number $n$ for (*a*) compounds **1**, (*b*) **2**, (*c*) **3**, (*d*) **4**: (○) layer spacing, (■) molecular length. In (*a*) ● indicates a reflection maximum observed in the N phase; in (*b*) ○ and ◇ are the layer spacings at low and high temperatures, respectively.

subtle change of the distribution ratio within the narrow temperature range is responsible for the complex phase transition behavior [12, 13, 16]. The reflection peaks at *c*. 30 and 60 Å arise from the $SmA_1$ and bilayer ($SmA_2$) structure, respectively. The slope of 2.2 Å/$CH_2$ for the plot (○) in figure 12 (*b*) supports the bilayer arrangement model in figure 11 (*d*). The layer spacing of *c*. 40 Å observed in the high temperature region for octyloxy–decyloxy homologues is *c*. 1.3 times the molecular length, and is close to that of the conventional '$SmA_d$' phase illustrated in figure 11 (*c*) [2]. In conclusion, the SmA phase for **2** is a mixture of three layer structures, with distribution dependent on physical properties such as molecular shape and temperature. At higher temperatures, the layer structure in figure 11 (*c*) predominates. The co-existence of two kinds of layer structure was previously found in a binary mixture of two polar LC materials [19, 20].

Compounds **3** have one kind of layer structure as shown in figure 12 (*c*), where the layer spacing can be approximated as a straight line, giving a slope of $d$Å $= 1.49n + 20.1$, which intersects with that of the calculated molecular length at 21.5 Å corresponding to the diameter of the methoxy homologue. Although the slope is different from that of **1**, the SmA phase fundamentally has a monolayer structure; the $\Delta$ value is thus a function of the carbon number.

Compounds **4** have two kinds of layer structure. One has a spacing of *c*. 32 Å, which is 4–5 Å longer than the calculated molecular length, and the plot gives $d$Å $= 1.55n + 19.8$. The layer structure is formed particularly in the lower temperature region, and the spacing is almost independent of temperature. From these results, the SmA phase is classified as $SmA_1$ one, having the layer structure shown in figure 11 (*b*). The other structure has a spacing of *c*. 40 Å, and exists only in the higher temperature region. The ratio of the layer spacing to the calculated molecular length is *c*. 1.4, similar to those of 4-cyanobiphenyl and 4-cyanophenyl benzoate compounds [2]. Therefore this SmA phase is classified as $SmA_d$. As we can see from figure 10, the $SmA_d$–$SmA_1$ transition is expected to occur in the range 160–150°C, although the phase transition could not be observed by either DSC or microscopy. There is no doubt that both layer structures co-exist in the SmA phase, and the distribution ratio is a function of temperature.

From these results, the $SmA_1$ phase in figure 11 (*b*) is assumed to be common through all the compounds, with the $\Delta$ value depending on the physical properties of the LC core portion.

Up to now, the anti-parallel model shown in figure 11 (*c*) has been frequently used as the model arrangement in the polar SmA phase, where two dipoles arising from the ester groups have been supposed to facilitate the layer arrangement. The orientation of the two ester groups for **1** and **2** is just the case, as shown in figure 11 (*a*), where two ester groups arrange anti-parallel side by side, so that the attractive interaction model appears to be very convincing. Certainly, the smectic properties are notably influenced by the relative orientation of the two ester groups with respect to the terminal alkoxy and polar groups in the present systems. However, the following facts are noteworthy. First, the distance between two ester groups is a function of the terminal alkoxy chain, as can be seen from figure 12 (*a*), so that two ester groups do not always arrange favourably. Second, in the '$SmA_d$' phase of the higher homologues of **4**, two ester groups inevitably arrange parallel in the model in figure 11 (*c*). Third, in the model structure of the $SmA_2$ phase in figure 11 (*d*) adjacent ester groups inevitably arrange parallel, whichever way the ester groups orient. In practice, however, the layer structure in figure 11 (*d*) is seen in the homologues of **2**.

Consequently, the diversity of the smectic properties for the ester compounds is less so easy to explain in terms of attractive interactions around the carbonyl groups. In this connection, we want to emphasize the relative importance of a subtle difference in molecular shape due to alternation of the ester groups. For example, we believe that the difference in mesomorphic properties between the pairs of compounds in figure 13 is essential for the diversity of smectic properties of ester compounds [14, 21]. The subtle difference in the molecular shape between these two pairs is apparently responsible for the diversity of smectic properties.

For the formation of the smectic layer in figure 1, furthermore, we wish to emphasize the importance of an affinity between polar and non-polar segments. The present compounds consist of three parts: that is, nitrobenzene, aromatic core, and alkoxy chain. It is important that nitrobenzene has low affinity (solubility) for hydrocarbon solvents such as hexane, heptane, etc. The mixture of nitrobenzene and the hydrocarbon solvents appears to be soluble at room temperature, but easily shows a phase separation on decreasing the temperature. These results suggest that nitrobenzene and also benzonitrile are intrinsically immiscible with hydrocarbon solvents. A similar phase separation should take place with the higher homologues of polar LC materials. Thus, in the present molecules, nitrobenzene moieties are easy separated from the hydrocarbon moiety and condense to form a smectic layer boundary in the LC states. The repulsive interaction between the polar and non-polar moieties should provide the driving force for the evolution of the layer structure shown in figure 1, i.e. $SmA_1$ and/or $SmA_d$ phases.

## 4. Conclusion

Four isomeric compounds having a terminal nitro group have marked smectogenic properties, and the layer structure of the SmA phase is strongly influenced by the relative orientation of their two ester groups with respect to terminal nitro and alkoxy groups, and by the alkoxy chain length. Not only the change in dipole moment but also a subtle change in the entire molecular shape are considered to be important factors for the diversity of the smectic properties. We would emphasize that polar and/or non-polar interactions at the surface of smectic layers are important factors in determining the physical properties of the smectic phases.

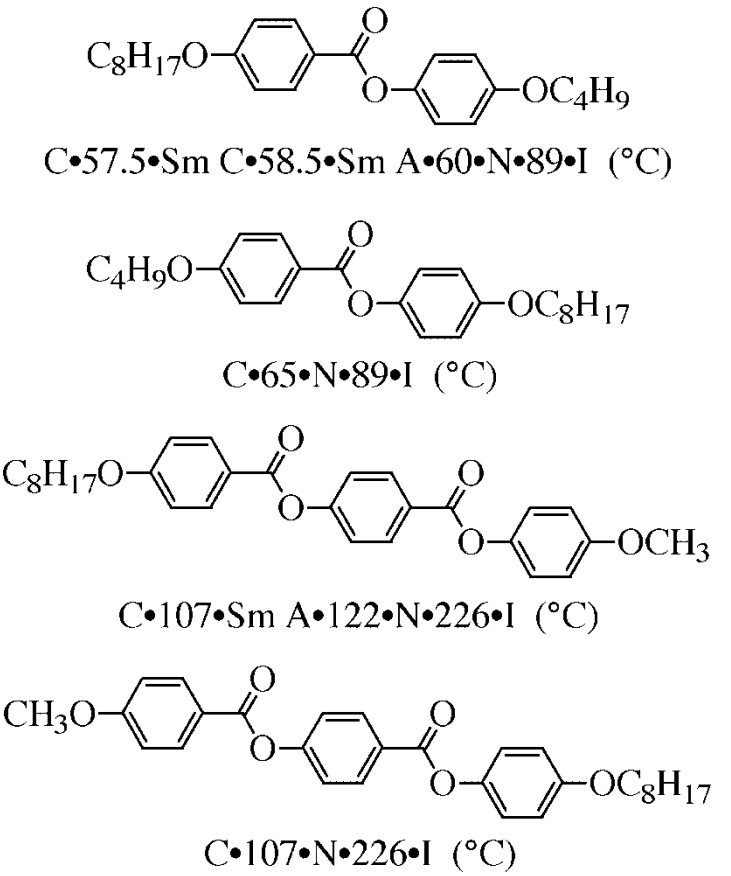


Figure 13. Isometic pairs with reversed ester configuration.



## References


[1] DUAN, M., TASAKA, T., OKAMOTO, H., and TAKENAKA S., 2000, *Liq. Cryst.*, **27,** 1195.

[2] CLADIS, P. E., 1998, *Liq. Cryst*., **24**, 15 and references cited therein.

[3] GOODBY, J. W., 1998, *Handbook of Liquid Crystals*, **Vol. 2A**, edited by D. Demus, J. Goodby, G. W. Gray, H.-W. Speiss and V. Vill (Weinheim: VCH), p.3.

[4] TASAKA, T., PETROV, V. F., OKAMOTO, H., MORITA, Y., SUETAKE, K., and TAKENAKA, S., 2002, *Liq. Cryst.*, **29,** 1311.

[5] SAKURAI, Y., TAKENAKA, S., SUGIURRA, H., and KUSABAYASHI, S., 1991, *Mol. Cryst. liq. Cryst.*, **201,** 95.

[6] RATNA, B. R., PRASAD, S. K., SHASHIDHAR, R., HEPPKE, G., and PFEIFFER, S., 1985, *Mol. Cryst. liq. Cryst.*, **124,** 21.

[7] NGUYEN, H. T., HARDOUIN, F., and DESTRADE, C., 1982, *J. Phys.*, **43,** 1127.

[8] NGUYEN, H. T., 1985, *Mol. Cryst. liq. Cryst.*, **127,** 143.

[9] HARDOUIN, F., NGUYEN, H. T., ACHARD, M. F., and LEVELUT, A. M., 1982, *J. Phys. Lett.*, **43,** L-327.

[10] HAUDOUIN, F., SIGAUD, G., NGUYEN, H. T., and ACHARD, M. F., 1981, *J. Phys., Lett.*, **42,** L-63.

[11] NOUNESIS, G., BLUM, K. I., YOUNG, M. J., GARLAND, C. W., and BIRGENEAU, R. J., 1993, *Phys. Rev. E*, **47,** 1910.

[12] SHASHIDHAR, R., RATNA, B. R., SURENDRANATH, V., RAJA, V. N., PRASAD, S. K., and NAGABHUSHAN, C., 1985, *J. Phys. Lett.*, **46,** L-445.

[13] FONTES, E., HEINEY, P. A., HASELTINE, J. L., and SMITH III, A. B., 1986, *J. Phys.*, **47,** 1533.

[14] TASAKA, T., OKAMOTO, H., PETROV, V. F., and TAKENAKA, S., 2001, *Liq. Cryst.*, **28,** 1025.

[15] MCMILLAN, W. L., 1973, *Phys. Rev. A*, **8,** 1921.

[16] HARDOUIN, F., ACHARD, M. F., NGUYEN, H. T., and SIGAUD, G., 1986, *Mol. Cryst. liq. Cryst.*, **3,** 7.

[17] SHASHIDHAR, R., RATNA, B. R., and KRISHNA PRASAD, S., 1984, *Mol. Cryst. liq. Cryst.*, **102,** 105.

[18] CLADIS, P. E., FINN, P. L., and GOODBY, J. W., 1978, *Liquid Crystals and Ordered Fluids*, **Vol. 3**, edited by J. F. Johnson and R. S. Porter (New York: Plenum Press), p.20.

[19] NISHIHATA, Y., SAKASHITA, H., TERAUCHI, H., TAKENAKA, S., and KUSABAYSHI, S., 1986, *J. phys. Soc, Jpn.*, **55,** 853.

[20] PATEL, P., CHEN, L., and KUMAR, S., 1993, *Phys. Rev. E.*, **47,** 2643.

[21] DEMUS, D., and ZASCHKE, H., 1976, *Flüssige Kristalle in Tabellen* **Vol. 1**, (Leipzig: VEB Deutscher Verlag für Grundstoff Industrie).